

Impedance Characteristics of Multi-Layer Grids

The power distribution network spans many layers of interconnect with disparate electrical properties. The impedance characteristics of multi-layer power distribution grids and the relevant design implications are the subject of this chapter.

Decoupling capacitors are an effective technique to reduce the effect of the inductance on power distribution networks operating at high frequencies. The efficacy of decoupling capacitors depends on the impedance of the conductors connecting the capacitors to the power load and source. The optimal allocation of the on-chip decoupling capacitance depends on the impedance characteristics of the interconnect. Robust and area efficient design of multi-layer power distribution grids therefore requires a thorough understanding of the impedance properties of the power distributing interconnect structures.

Power distribution networks in high performance digital ICs are commonly structured as a multi-layer grid, as shown in Fig. 13.1. The inductive properties of single layer power grids have been described in Chapter 9. In grid layers with alternating power and ground lines, long distance inductive coupling is greatly diminished due to cancellation, turning inductive coupling in single layer power grids into, effectively, a local phenomenon. The grid inductance, therefore, behaves similarly to the grid resistance: increases linearly with grid length and decreases inversely linearly with grid width (*i.e.*, the number of lines in the grid). The electrical properties of power distribution grids can therefore be conveniently expressed by a dimension-independent sheet resistance R_{\square} and sheet inductance L_{\square} [276]. The inductance of the power grid layers can be efficiently estimated using simple models comprised of a few interconnect lines.

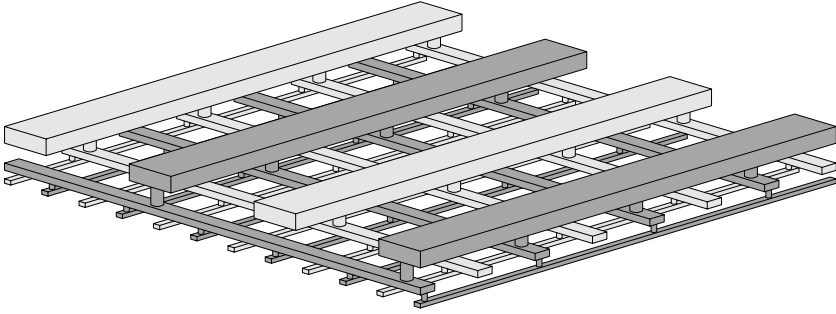


Fig. 13.1. A multi-layer power distribution grid. The ground lines are light grey, the power lines are dark grey.

Area/inductance/resistance tradeoffs in power distribution grids have also been investigated in Chapter 11. The sheet inductance of power distribution grids is shown to increase linearly with line width under two different tradeoff scenarios. Under the constraint of constant grid area, a tradeoff exists between the grid inductance and resistance. Under the constraint of a constant grid resistance, the grid inductance can be traded off against grid area.

The variation of inductance with frequency in single layer power grids has been characterized in Chapter 10. This variation is relatively moderate, typically less than 10% of the low frequency inductance. An exception from this behavior is power grids with closely spaced power and ground lines where the inductance variation with frequency is greater due to significant proximity effects.

Power distribution grids in modern integrated circuits typically consist of many grid layers, spanning an entire stack of interconnect layers. The objective of the present investigation is to characterize the electrical properties of these multi-layer grids, advancing the existing work beyond individual grid layers.

The chapter is organized as follows. The impedance characteristics of multi-layer power distribution grids are discussed in Section 13.1. A case study of a two layer power grid is presented in Section 13.2. The design implications of the impedance properties of a multi-layer grid are discussed in Section 13.3. The chapter concludes with a summary.

13.1 Electrical properties of multi-layer grids

A circuit model of multi-layer power distribution grids is developed in this section. The impedance characteristics of multi-layer grids are determined based on this model. The impedance characteristics of individual layers of multi-layer power distribution grids are discussed in Section 13.1.1. The variation with frequency of the impedance characteristics of several grid layers forming a multi-layer grid is analyzed in Section 13.1.2.

13.1.1 Impedance characteristics of individual grid layers

The power and ground lines within each layer of a multi-layer power distribution grid are orthogonal to the lines in the adjacent layers. Orthogonal lines have zero mutual partial inductance as there is no magnetic linkage [42]. Orthogonal grid layers can therefore be evaluated independently. A multi-layer grid can be considered to consist of two stacks of layers, with all of the lines in each stack parallel to each other, as shown in Fig. 13.2. Grid lines in one stack are orthogonal to the lines in the other stack. Grid layers in each stack only affect the grid inductance in the direction of the lines in the stack. This behavior is analogous to the properties of the grid resistance. The problem of characterizing a multi-layer grid is thereby reduced to determining the impedance characteristics of a stack of several individual grid layers with lines in the same direction.

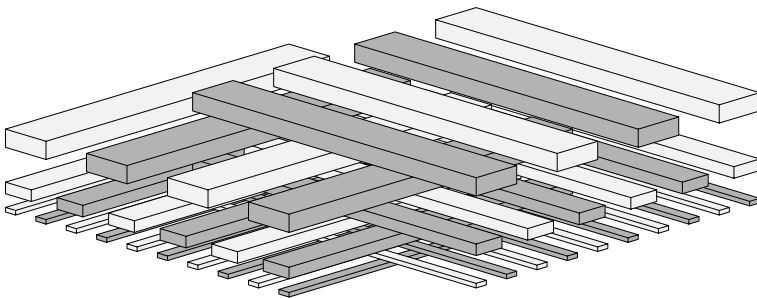


Fig. 13.2. A multi-layer grid consists of two stacks of layers. The lines in each stack are parallel to each other. The layers in one stack determine the resistive and inductive characteristics of the multi-layer grid in the direction of the lines in that stack, while the layers in the other stack determine the impedance characteristics in the orthogonal direction.

The power and ground lines in power distribution grids are connected to the lines in the adjacent layers through vias. The vias (or clusters of vias) are distributed along a power line at a pitch equal to the power line pitch in the adjacent layer. The line pitch is much larger than the via length. The inductance and resistance of the two close parallel power lines in different metal layers are therefore much larger than the resistance and inductance of the connecting vias. The effect of vias on the resistance and inductance of a power grid is therefore negligible. This property is a direct consequence of the characteristic that the distance of the lateral current distribution in power grids (hundreds or thousands of micrometers) is much larger than the distance of the vertical current distribution (several micrometers). The power current is distributed among the metal layers over a distance comparable to a line pitch. The power and ground lines are effectively connected in parallel.

Each layer of a typical multi-layer power distribution grid has significantly different electrical properties. Lines in the upper layers tend to be thick and wide, forming a low resistance global power distribution grid. Lines in the lower layers tend to be thinner, narrower, and have a smaller pitch. The lower the metal layer, the smaller the metal thickness, width, and pitch. The upper grid layers therefore have a relatively high inductance and low resistance, whereas the lower layers have a relatively low inductance and high resistance [70], [276]. The lower the layer, the higher the resistance and the lower the inductance. In those circuits employing flip-chip packaging with a high density area array of I/O contacts, the interconnect layers in the package are tightly coupled to the on-chip interconnect, effectively extending the on-chip interconnect hierarchy. The difference in the electrical properties across the interconnect hierarchy is particularly significant in nanoscale circuits. While the cross-sectional dimensions of local on-chip lines are measured in tens of nanometers, the dimensions of package lines are of the order of tens of micrometers. The three orders of magnitude difference in dimensions translates to six orders of magnitude difference in resistance (proportional to the cross-sectional area of the grid lines) and to three orders of magnitude difference in inductance (proportional to the grid line density).

The variation with frequency of the impedance of each layer in a grid stack comprised of N grid layers is schematically shown in Fig. 13.3. The layers are numbered from 1 (the uppermost layer) to N (the

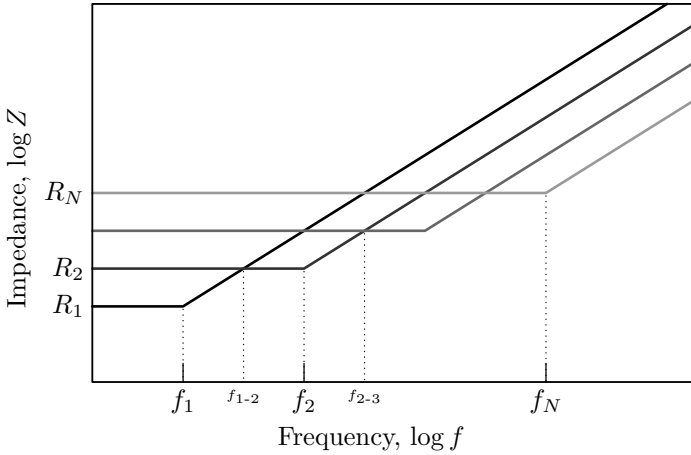


Fig. 13.3. Impedance of the individual grid layers comprising a multi-layer grid.

lowest layer). The grid layer resistance increases with layer number, $R_1 < R_2 < \dots < R_N$, and the inductance decreases with layer number $L_1 > L_2 > \dots > L_N$. At low frequencies, the uppermost layer has the lowest impedance as the layer with the lowest resistance. This layer, however, has the highest inductance and, consequently, the lowest transition frequency $f_1 = \frac{1}{2\pi} \frac{R_1}{L_1}$, as compared to the other layers (see Fig. 13.3). The transition frequency is the frequency at which the impedance of the grid layer changes in character from resistive to inductive. At this frequency, the inductive impedance of a grid layer is equal to the resistive impedance (neglecting skin and proximity effects), *i.e.*, $R_1 = \omega L_1$. The grid impedance increases linearly with frequency above f_1 . The lowest grid layer has the highest resistance and the lowest inductance; therefore, this layer has the highest transition frequency f_N . As the inductance of the upper layers is higher than the lower layers, the impedance of an upper layer exceeds the impedance of any lower layer above a certain frequency. For example, the impedance of the first layer $R_1 + \omega L_1 \approx \omega L_1$ equals the magnitude of the second layer impedance $R_2 + \omega L_2 \approx R_2$ and exceeds the impedance of the second layer above frequency $f_{1-2} = \frac{1}{2\pi} \frac{R_2}{L_1}$, as shown in Fig. 13.3. Similarly, the impedance of layer k exceeds the impedance of layer l , $k < l$, at $f_{k-l} = \frac{1}{2\pi} \frac{R_l}{L_k}$.

13.1.2 Impedance characteristics of multi-layer grids

An entire stack of grid layers cannot be accurately described by a single RL circuit due to the aforementioned differences among the electrical properties of the individual grid layers. A stack of multiple grid layers can, however, be modeled by several parallel RL branches, each branch characterizing the electrical properties of one of the comprising grid layers, as shown in Fig. 13.4.

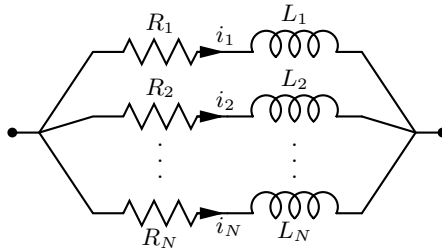


Fig. 13.4. Equivalent circuit of a stack of N grid layers.

Due to the difference in the electrical properties of the individual layers, the magnitude of the current in each grid layer varies significantly with frequency. At low frequencies, the low resistance uppermost layer is the path of lowest impedance, as shown in Fig. 13.3. The uppermost layer has the greatest effect on the low frequency resistance and inductance of the grid stack, as the largest share of the overall current flows through this layer. As the frequency increases to $f_{1-2} = \frac{1}{2\pi} \frac{R_2}{L_1}$ and higher, the impedance of the uppermost layer ωL_1 exceeds the impedance of the second uppermost layer R_2 , as shown in Fig. 13.3. The second uppermost layer, therefore, carries the largest share of the overall current and most affects the inductance and resistance within this frequency range. As the frequency exceeds $f_{2-3} = \frac{1}{2\pi} \frac{R_3}{L_2}$, the next layer in the stack becomes the path of least impedance and so on. The process continues until at very high frequencies the lowest layer carries most of the overall current.

As the frequencies increase, the majority of the overall current is progressively transferred from the layers of low resistance and high inductance to the layers of high resistance and low inductance. The overall grid inductance, therefore, decreases with frequency and the overall grid resistance increases with frequency. A qualitative plot of the variation of the grid inductance and resistance with frequency is shown in

Fig. 13.5. At low frequency, all of the layers exhibit a purely resistive behavior and the current is partitioned among the layers according to the resistance of each layer. The share i_k of the overall current flowing through layer k is

$$i_k = \frac{I_k}{\sum_{n=1}^N I_n} = \frac{\prod_{n \neq k} R_n}{\sum_{m=1}^N \prod_{n \neq m} R_n}. \tag{13.1}$$

Note that $i_1 > i_2 > \dots > i_N$ as $R_1 < R_2 < \dots < R_N$. The resistance of a multi-layer grid R_0^{LF} at low frequency is therefore determined by the parallel connection of all of the individual layer resistances,

$$R_0^{LF} = R_1 \parallel R_2 \parallel \dots \parallel R_N = \frac{\prod_{n=1}^N R_n}{\sum_{m=1}^N \prod_{n \neq m} R_n}. \tag{13.2}$$

The low frequency inductance of a multi-layer grid L_0^{LF} is, however,

$$L_0^{LF} = L_1 i_1^2 + L_2 i_2^2 + \dots + L_N i_N^2 \approx L_1, \tag{13.3}$$

due to $L_1 > L_k$ and $i_1 > i_k$ for any $k \neq 1$.

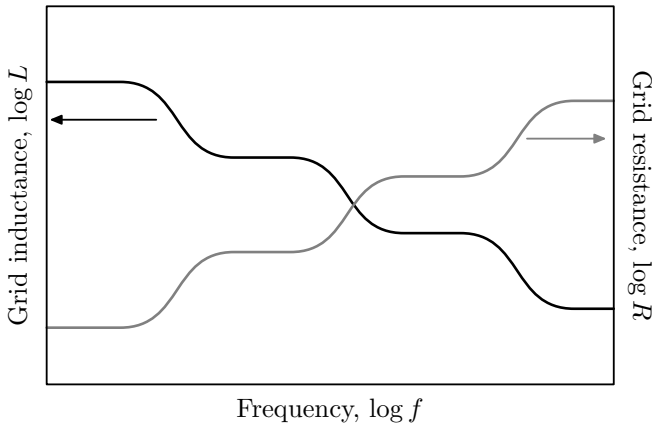


Fig. 13.5. Variation of the grid inductance and resistance of a multi-layer stack with frequency. As the signal frequency increases, the current flow shifts to the high resistance, low inductance layers, decreasing the inductance and increasing the resistance of the grid.

At very high frequencies, the resistance and inductance exchange roles. All of the grid layers exhibit a purely inductive behavior and the

current is partitioned among the layers according to the inductance of each layer. The share of the overall current flowing through layer n is

$$i_k = \frac{I_k}{\sum_{n=1}^N I_n} = \frac{\prod_{n \neq k} L_n}{\sum_{m=1}^N \prod_{n \neq m} L_n}. \quad (13.4)$$

The relation among the currents of each layer is reversed as compared to the low frequency case: $i_1 < i_2 < \dots < i_N$. The inductance of a multi-layer grid at high frequency L_0^{HF} is determined by the parallel connection of the individual layer inductances,

$$L_0^{HF} = L_1 \parallel L_2 \parallel \dots \parallel L_N = \frac{\prod_{n=1}^N L_n}{\sum_{m=1}^N \prod_{n \neq m} L_n}. \quad (13.5)$$

The high frequency resistance of a multi-layer grid R_0^{HF} is

$$R_0^{HF} = R_1 i_1^2 + R_2 i_2^2 + \dots + R_N i_N^2 \sim R_N, \quad (13.6)$$

due to $R_N > R_k$ and $i_N > i_k$ for any $k \neq N$.

The grid resistance and inductance vary with frequency between these limiting low and high frequency cases. If the difference in the electrical properties of the layers is sufficiently high, the variation of the grid inductance and resistance with frequency has a staircase-like shape, as shown in Fig. 13.5. As the frequency increases, the grid layers consecutively serve as the primary current path, dominating the overall grid impedance within a specific frequency range [291].

13.2 Case study of a two layer grid

The electrical properties of a two layer grid are evaluated in this section to quantitatively illustrate the concepts described in Section 13.1. The grid parameters are described in Fig. 13.6.

The analysis approach used to determine the electrical characteristics of a grid structure is described in Section 13.2.1. Magnetic coupling between grid layers is discussed in Section 13.2.2. The inductive characteristics of a two layer grid are discussed in Section 13.2.3. The resistive characteristics of a two layer grid are discussed in Section 13.2.3. The impedance characteristics of a two layer grid are summarized in Section 13.2.5.

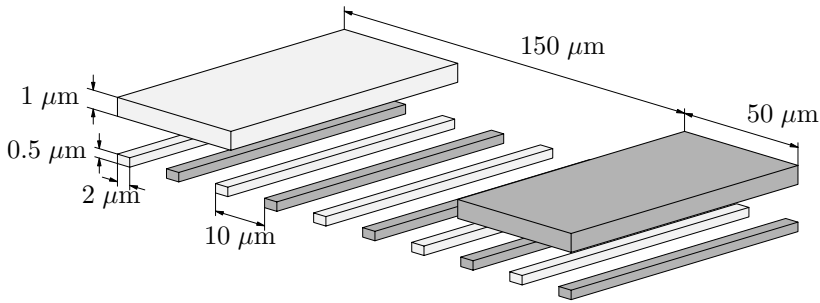


Fig. 13.6. General view of a two layer grid. The ground lines are white colored, the power lines are grey colored.

13.2.1 Simulation setup

The inductance extraction program FastHenry [67] is used to explore the inductive properties of grid structures. FastHenry efficiently calculates the frequency dependent impedance $R(\omega) + \omega L(\omega)$ of complex three-dimensional interconnect structures under a quasi-magnetostatic approximation. In the analysis, the lines are split into multiple filaments to account for skin and proximity effects, as discussed in Section 2.2. A conductivity of $58 \text{ S}/\mu\text{m} \simeq (1.72 \mu\Omega \cdot \text{cm})^{-1}$ is used in the analysis where an advanced process with copper interconnect is assumed [275].

When determining the loop inductance, all of the ground lines at one end of the grid are short circuited to form a ground terminal and all of the power lines at the same end of the grid are short circuited to form a power terminal. All of the lines at the other end of the grid are short circuited to complete the current loop. This configuration assumes that the power current loop is completed on-chip. This assumption is valid for high frequency signals which are effectively terminated through the on-chip decoupling capacitance which acts as a low impedance termination as compared to the inductive off-chip leads of the package. If the current loop is completed on-chip, the current in the power lines and the current in the ground lines always flow in opposite directions.

13.2.2 Inductive coupling between grid layers

An equivalent circuit diagram of a two layer power distribution grid is shown in Fig. 13.7. The partial mutual inductance between the lines in the two grid layers is significant as compared to the partial self inductance of the lines. Therefore, the two grid layers are, in general,

magnetically coupled, as indicated in Fig. 13.7. It can be shown, however, that for practical geometries, magnetic coupling is significant only in interdigitated grids under specific conditions.

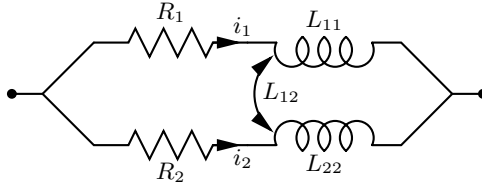


Fig. 13.7. An equivalent circuit diagram of a two layer grid.

The specific conditions are that the line pitch in both layers is the same and the separation between the two layers is smaller than the line pitch. The two layers with the same line pitch are spatially correlated, *i.e.*, the relative position of the lines in the two layers is repeated throughout the structure. The net inductance of such grids depends upon the mutual alignment of the two grid layers. For example, consider a two layer grid with each layer consisting of ten interdigitated power and ground lines with a $1\ \mu\text{m} \times 1\ \mu\text{m}$ cross section on an $8\ \mu\text{m}$ pitch, as in the cross section shown in Fig. 13.8. The separation between the layers is $4\ \mu\text{m}$. The variation of inductance of this two layer grid structure as a function of the physical offset between the two layers is shown in Fig. 13.9.

At 1 GHz, each of the layers has a loop inductance of 206 pH. The inductance of two identical parallel coupled inductors is

$$L_{1\parallel 2} = \frac{L_{11}L_{22} - L_{12}^2}{L_{11} + L_{22} - 2L_{12}} = \frac{L_{11} + L_{12}}{2}. \quad (13.7)$$

In the case of zero coupling between the two grid layers, the net inductance of the two layer grid is approximately $206\ \text{pH}/2 = 103\ \text{pH}$ since the two grids are in parallel. If the ground lines in the top layer are placed immediately over the power lines of the bottom layer, as shown in Fig. 13.8(a), a close return path for the power lines is provided as compared to the neighboring ground lines of the bottom layer. The magnetic coupling between the two grid layers is negative in this case, resulting in a net inductance of 81 pH for the two layer grid (which is lower than the uncoupled case of 103 pH), in agreement with (13.7). A two layer interdigitated grid effectively becomes a paired grid, as shown

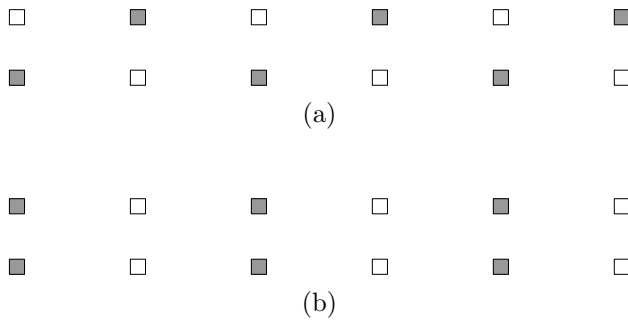


Fig. 13.8. Alignment of two layers with the same line pitch in a two layer grid resulting in the minimum and maximum grid inductance. The ground lines are white colored, the power lines are grey colored. a) The configuration with the minimum grid inductance: ground lines of one layer are aligned with the power lines of the other layer. b) The configuration with the maximum grid inductance: the ground lines of both layers are aligned with each other.

in Fig. 13.8(a). (Rather than equidistant line spacing, in paired grids the lines are placed in close power-ground line pairs [69].) If, alternatively, the ground lines of the top layer are aligned with the ground lines of the bottom layer, as shown in Fig. 13.8(b), the magnetic coupling between the two layers is positive and the net inductance of the two layer grid is 124 pH, higher than the uncoupled case, also in agreement with (13.7). As the offset between the grid layers changes between these two limits, the total inductance varies from a minimum of 81 pH to a maximum of 124 pH, passing a point where the effective coupling between the two layers is zero and the total inductance is 103 pH. The inductance at a 100 GHz signal frequency closely tracks this behavior at low frequencies.

If the layer separation is greater than the line pitch in either of the two layers, the net coupling from the lines in one layer to the lines in the other layer is insignificant. Coupling to the power lines is nearly cancelled by the coupling to the ground lines, carrying current in the opposite direction. This coupling cancellation is analogous to the cancellation of the long distance coupling within the same grid layer [69]. This cancellation also explains why two grid layers are effectively uncoupled if one of the layers is a paired grid. The power to ground line separation in a paired grid is smaller than the separation between two metalization layers with the grid lines in the same direction.

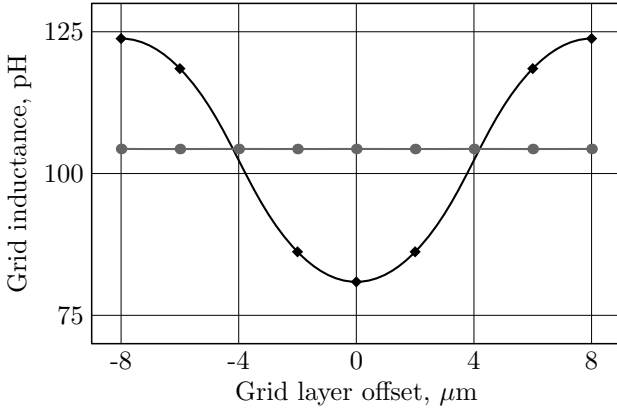


Fig. 13.9. Inductance of a two layer grid versus the physical offset between the two layers. The inductance of the grid with matched line pitch of the layers (black line) depends on the layer offset. (The low inductance alignment shown in Fig. 13.8(a) is chosen as the zero offset.) The inductance of the grid is constant where the line height, width, and pitch of the lower layer are twice as small as compared to the upper layer (the gray line).

It is possible to demonstrate that in the case where the line pitch is not matched, as shown in Fig. 13.10, the layer coupling is effectively cancelled, and the grid inductance is independent of the layer alignment, as shown in Fig. 13.9. Metalization layers in integrated circuits typically are of different thickness, line width, and line spacing. Therefore, unless intentionally designed otherwise, different grid layers typically have different line pitch and can be considered uncoupled, as has been implicitly assumed in Section 13.1.



Fig. 13.10. The cross section of a two layer grid with the line pitch of the upper layer a fractional multiple ($5/4$ in the case shown) of the line pitch in the bottom layer. Both effects illustrated in Fig. 13.8 occur at different locations (circled). The ground lines are white colored, the power lines are grey colored.

13.2.3 Inductive characteristics of a two layer grid

The variation of the sheet inductance with signal frequency in the two layer grid is shown in Fig. 13.11. Note that the inductance of the individual grid layers, also shown in Fig. 13.11, is virtually constant with frequency [69], [277]. The sheet inductance of the upper layer L_1 is 268 pH/□ at 1 MHz (247 pH/□ at 100 GHz). The sheet inductance of the bottom layer L_2 is 19.6 pH/□ at 1 MHz (19 pH/□ at 100 GHz). The inductance of the bottom grid layer is approximately fifteen times lower than the inductance of the upper grid layer. This difference in inductance is primarily due to the difference in the line density of the layers. The line density of the bottom layer is fifteen times higher, as determined by the line pitch of the layers ($150/10 = 15$). The inductance of a single line is relatively insensitive to the aspect ratio of the line cross section. The inductance of the two layer grid, however, varies significantly with signal frequency due to current redistribution, as discussed in Section 13.1.

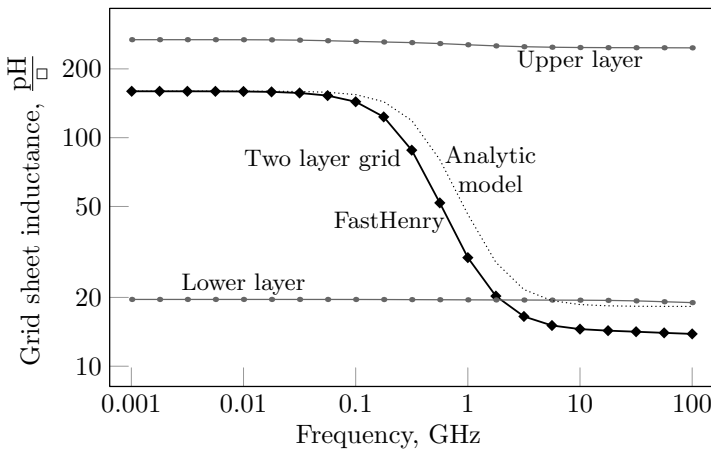


Fig. 13.11. Inductance of a two layer grid versus signal frequency. Both FastHenry data (solid line) and the analytic model data (dotted line) are shown. The individual inductance of the two comprising grid layers is shown for comparison (FastHenry data).

The inductive characteristics of a two layer grid can also be analytically determined based on the simple model shown in Fig. 13.7. Assuming $L_{12} = 0$ as discussed in Section 13.2.2, the loop inductance

of a two layer grid is

$$L_0 = \frac{L_1(R_2^2 + \omega^2 L_1 L_2) + L_2(R_1^2 + \omega^2 L_1 L_2)}{(R_1 + R_2)^2 + \omega^2 (L_1 + L_2)^2}. \quad (13.8)$$

At high frequencies, where the resistance of the grid layers has no influence on the current distribution between the layers, the grid inductance described by (13.8) asymptotically approaches the inductance of two ideal parallel inductors,

$$L_0^{HF} = \frac{L_1 L_2}{L_1 + L_2}, \quad (13.9)$$

in agreement with (13.5). At low frequencies, the grid inductance described by (13.8) approaches the low frequency limit of the grid inductance,

$$L_0^{LF} = L_1 \left(\frac{R_2}{R_1 + R_2} \right)^2 + L_2 \left(\frac{R_1}{R_1 + R_2} \right)^2 = 160 \text{ pH}/\square, \quad (13.10)$$

in agreement with (13.3).

The variation of the grid inductance with frequency according to the analytic model described by (13.8) is also illustrated in Fig. 13.11 by the dotted line. The analytic model satisfactorily describes the variation of grid inductance with frequency. The discrepancy between the analytic and FastHenry data at high frequencies is due to proximity effects which are not captured by the model shown in Fig. 13.7.

13.2.4 Resistive characteristics of a two layer grid

The resistance of the two individual grid layers R_1 and R_2 and the resistance of the combined two layer grid R_0 are shown in Fig. 13.12. The resistance of the individual grid layers remains constant up to high frequencies. The resistance of the upper layer begins to moderately increase from approximately 0.5 GHz due to significant proximity effects in very wide lines. The resistance of both layers sharply increases above approximately 20 GHz due to significant skin effect. Note that the resistance of the grid comprised of the two layers exhibits significantly greater variation with frequency than either individual layer.

Similar to the grid inductance, the resistive characteristics of a two layer grid can be analytically determined from the properties of the comprising grid layers,

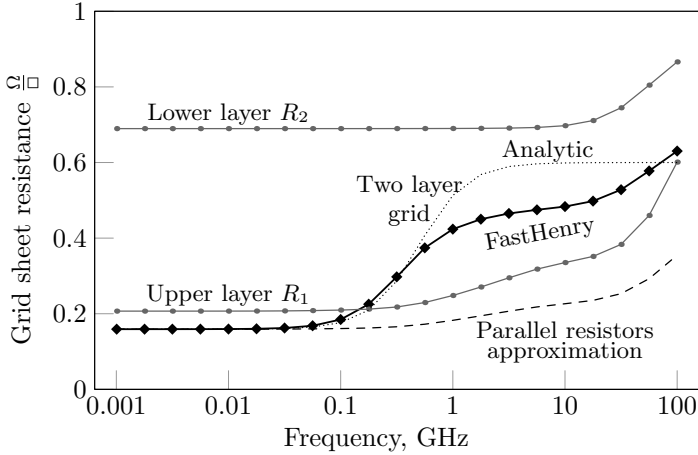


Fig. 13.12. Resistance of a two layer grid versus signal frequency. The individual resistance of the two comprising grid layers and the parallel resistance of the individual layer resistances are shown for comparison.

$$R_0 = \frac{R_1(R_1 R_2 + \omega^2 L_2^2) + R_2(R_1 R_2 + \omega^2 L_1^2)}{(R_1 + R_2)^2 + \omega^2(L_1 + L_2)^2}. \quad (13.11)$$

The grid resistance versus frequency data based on the analytic model described by (13.11) is shown by the dotted line in Fig. 13.12. The analytic solution describes well the general character of the resistance variation with frequency. At low frequencies, the resistance of the two layer grid approaches the parallel resistance of two grid layers,

$$R_0^{LF} = R_1 \parallel R_2 = \frac{R_1 R_2}{R_1 + R_2} = 0.16 \Omega/\square, \quad (13.12)$$

in agreement with (13.2). The high frequency grid resistance asymptotically approaches

$$R_0^{HF} = R_1 \left(\frac{L_2}{L_1 + L_2} \right)^2 + R_2 \left(\frac{L_1}{L_1 + L_2} \right)^2 = 0.6 \Omega/\square, \quad (13.13)$$

in agreement with (13.6). This analytically calculated high frequency resistance overestimates the FastHenry extracted resistance of $0.48 \Omega/\square$ (at 10 GHz). The discrepancy is due to pronounced proximity and skin effects at high frequencies.

13.2.5 Variation of impedance with frequency in a two layer grid

Having determined the variation with frequency of the resistance and inductance in the previous sections, it is possible to characterize the frequency dependent impedance characteristics of a two layer grid. The magnitude of the impedance calculated from the analytic models (13.8) and (13.11) is shown in Fig. 13.13 by the dotted line. Low frequency values of the individual layer inductance, L_1 and L_2 , and resistance, R_1 and R_2 , are used in the analytic model. The impedance magnitude based on FastHenry extracted data is shown by the solid line. The extracted impedance of the individual grid layers is also shown for comparison. Note that the impedance characteristics of the individual layers shown in Fig. 13.13 bear close resemblance to the schematic graph shown in Fig. 13.3.

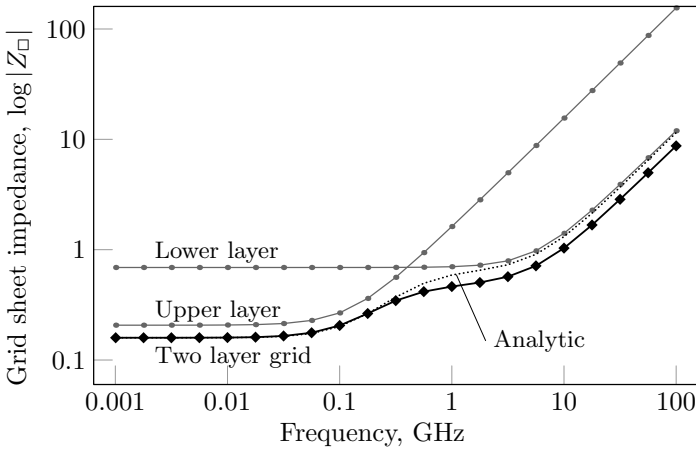


Fig. 13.13. Impedance magnitude of a two layer grid versus signal frequency. Both the extracted (solid line) and analytic (dotted line) data are shown. The impedance of the two comprising grid layers is also shown.

As discussed in Section 13.1, the low resistance upper grid dominates the impedance characteristics at low frequencies, while the low inductance lower grid determines the impedance characteristics at high frequencies [291]. The analytic model satisfactorily describes the frequency dependent impedance characteristics. The discrepancy

between the analytic and extracted data at high frequencies is due to overestimation of the high frequency inductance by the analytic model, as shown in Fig. 13.11.

13.3 Design implications

The variation with frequency of the electrical properties of a multi-layer grid has several design implications. Modeling the resistance of a multi-layer grid as a parallel connection of individual layer resistances underestimates the high frequency resistance of the grid. The parallel resistance model, therefore, underestimates the resistive IR voltage drops during fast current transients. Representing a multi-layer grid inductance by the individual layer inductances connected in parallel is accurate only at very high frequencies. At lower frequencies, this model underestimates the grid inductance. Relatively low inductance and high resistance at high frequencies increase the damping factor of the power distribution grid (proportional to R/\sqrt{L}), thereby preventing resonant oscillations in power distribution networks at high frequencies. Conversely, resonant oscillations are more likely at lower frequencies, where the inductance is relatively high and the resistance is low.

Multi-layer grids with different grid layer impedance characteristics are well suited to distribute power in high speed integrated circuits. At low frequencies, where the grid impedance is dominated by the resistance, most of the current flows through the less resistive upper grid layers, decreasing the grid impedance. At high frequencies, where the grid impedance is dominated by the inductance, most of the current flows through the low inductance lower layers. Over the entire frequency range, the current flow changes so as to minimize the impedance of the grid. These properties of multi-layer power distribution grids support the design of power distribution networks with low impedance across a wide frequency range, necessary in high performance nanoscale integrated circuits.

The inductive properties of the interconnect changes the metal allocation strategy for global power distribution grids. In circuits based on resistance-only models, all of the metal area for the global power distribution is allocated in the upper layers with the lowest line resistance. The power interconnect in the lower metal layers connects the circuits to the global power grid and typically do not form continuous power grids. In multi-layer grids, however, significant metal resources

are required to form continuous grids in the lower metal layers. This difference is a direct consequence of the inductive behavior of interconnect at high frequencies. A significant fraction of the high density lower metal layers should be used to lower the high frequency impedance of the power grid. In this manner, the frequency range of the grid impedance is extended to match the increased switching speeds of scaled transistors.

Redistribution of the grid current toward the lower layers at high frequencies increases the current density in the power and ground lines in the lower grid layers, degrading the electromigration reliability of the power distribution grid. The significance of these effects will increase as the frequency of the current delivered through the on-chip power distribution grid increases with higher operating speeds. An analysis of these effects is therefore necessary to ensure the integrity of high speed nanoscale integrated circuits.

13.4 Summary

The electrical characteristics of multi-layer power distribution grids are investigated in this chapter. The primary results are summarized as follows.

- The upper metal layers comprised of thicker and wider lines have low resistance and high inductance; the lower metal layers comprised of thinner and narrower lines have relatively high resistance and low inductance
- Inductive coupling between grid layers is shown to be insignificant in typical power distribution grids
- Due to this difference in electrical properties, the impedance characteristics of multi-layer grids vary significantly with frequency
- The current distribution among the grid layers changes with frequency, minimizing the overall impedance of the power grid
- As signal frequencies increase, the majority of the current flow shifts from the lower resistance upper layers to the lower inductance lower layers
- The inductance of a multi-layer grid decreases with frequency, while the resistance increases with frequency

- An analytic model describing the electrical properties of a multi-layer grid based on the inductive and resistive properties of the comprising grid layers is described
- A dense and continuous power distribution grid in the lower metal layers is essential to reduce the impedance of a power distribution grid operating at high frequencies